

# OBSERVATION OF ENERGY TRANSFER BETWEEN IDENTICAL-FREQUENCY LASER BEAMS IN A FLOWING PLASMA

*K. B. Wharton\**

*B. B. Afeyan\*\**

*R. K. Kirkwood*

*B. I. Cohen*

*S. H. Glenzer*

*J. D. Moody*

*K. G. Estabrook*

*C. Joshi†*

## Introduction

Energy transfer between two intersecting laser beams in a plasma directly addresses fundamental aspects of laser-plasma interactions and is also relevant to laser-driven inertial confinement fusion (ICF). When an electromagnetic wave (frequency  $\omega_0$ , wave number  $\mathbf{k}_0$ ) intersects another electromagnetic wave with equal or lower frequency ( $\omega_1$ ,  $\mathbf{k}_1$ ), optical mixing will drive a beat-wave density perturbation in the plasma at  $(\Omega, \mathbf{K})$ :

$$\Omega = \omega_0 - \omega_1; \mathbf{K} = \mathbf{k}_0 - \mathbf{k}_1. \quad (1)$$

If the driven beat-wave satisfies the plasma-dispersion relation, then this three-wave interaction is resonant and can be very efficient.<sup>1,2</sup> Electron plasma waves can be driven in this manner, using two laser beams with a difference in frequency equal to the electron plasma frequency.<sup>1,3</sup> This technique has found applications in particle acceleration.<sup>4-6</sup> For beams of comparable frequency, resonance can be reached when  $(\Omega, \mathbf{K})$  satisfies the dispersion relation  $(\Omega = \omega_{ia}, \mathbf{K} = \mathbf{k}_{ia}) = 0$  for ion-acoustic waves in a flowing plasma:

$$\omega_{ia} = c_s |\mathbf{k}_{ia}| + \mathbf{v}_d \cdot \mathbf{k}_{ia}. \quad (2)$$

Here  $c_s$  is the ion sound speed, and  $\mathbf{v}_d$  is the drift velocity of the plasma. In subsonic plasmas ( $|\mathbf{v}_d| < c_s$ ), Eq. 1 and Eq. 2 show that identical frequency beams cannot drive a resonant ion wave. With the appropriate frequency mismatch, however, resonant ion waves have been driven by microwaves<sup>7</sup> and also by two

laser beams.<sup>8</sup> This latter experiment measured a modest transfer of energy mediated by a resonant ion wave, as evidenced by the fact that no energy transfer was observed for two laser beams of equal frequency.

Nonresonant ion waves have been produced with two identical frequency beams, which were found to have an effect on stimulated Raman scattering.<sup>9</sup> More recently, Lal et al. have observed energy transfer between two  $\lambda = 10.6\text{-}\mu\text{m}$ -wavelength laser beams,<sup>10</sup> but this was during a transient period on the order of a few acoustic periods, during which energy transfer may occur between identical frequency beams.<sup>11,12</sup> These previous experiments were performed in subsonic plasmas. In a supersonic plasma ( $|\mathbf{v}_d| \geq c_s$ ) the resonant ion wave can have zero frequency in the laboratory frame if  $\omega_{ia} = 0$  in Eq. 2, and the ion wave can therefore transfer energy between two identical frequency beams over many acoustic periods.<sup>13-15</sup> In this article, we present the first measurements of steady-state energy transfer between identical frequency beams in a plasma with supersonic flow.

This effect has been the subject of much theoretical work,<sup>12,16,17</sup> in part motivated by current designs for fusion experiments on the National Ignition Facility<sup>18</sup> (NIF) in which multiple laser beams cross as they enter a cylindrical radiation enclosure (hohlraum). Because the plasma flow leaving the enclosure is near supersonic,<sup>15</sup> there may be resonant energy exchange between the laser beams. This would have deleterious effects on the symmetry of the laser radiation inside the hohlraum and might require the use of the NIF's ability to frequency detune the crossed beams and avoid a resonance.

## Experimental Configuration

The experiments were performed on the 10-beam Nova laser facility at Lawrence Livermore National Laboratory (LLNL), using four  $f/4.3$  beams with

\*University of California, Los Angeles, Los Angeles, CA, and Lawrence Livermore National Laboratory, Livermore, CA

\*\*Polymath Associates, Livermore, CA, and University of Nevada, Reno, Reno, NV

†University of California, Los Angeles, Los Angeles, CA

$\lambda = 351$  nm. Two of the beams were partially defocused to 80- $\mu\text{m}$ -diam spots, each spatially smoothed with a kinoform phase plate<sup>19</sup> (KPP) and each containing 3 kJ of energy in a square pulse lasting from  $t = 0$  to  $t = 3$  ns. These two heater beams were incident ( $40^\circ$  to normal) on both sides of a 5- $\mu\text{m}$ -thick Be ( $Z = 4$ ) rectangular foil, 2 mm by 4 mm. The exploding foil was initially modeled with LASNEX,<sup>20</sup> using the heater beam parameters described above. A layer with Mach 1 flow ( $|\mathbf{v}_d| = c_s$ ) was calculated to move out from the initial foil position over time, reaching a distance of 500  $\mu\text{m}$  from the foil at  $t = 3$  ns. At this time, the density along the center normal of the foil had reached a 1-mm-scale plateau of a roughly constant electron density  $n_e = 0.06 n_c$ , where  $n_c$  is the critical density for 351-nm light ( $9 \times 10^{21} \text{ cm}^{-3}$ ).

The flow velocity was experimentally characterized with a Thomson scattering technique.<sup>21</sup> A lower-intensity,  $\lambda = 526$ -nm beam was focused in a 100- $\mu\text{m}$  full-width at half maximum (FWHM) spot, 500  $\mu\text{m}$  from the center foil position. The frequency- and time-resolved Thomson scattered light is shown in Figure 1a. At  $t = 2.9$  ns, the upshifted ion wave feature overlaps the stray light, signifying that  $\omega_{ia} = 0$  and that a Mach 1 plasma flow was present. Figure 1b shows that this measured Mach 1 position ( $z = 500 \mu\text{m}$ ,  $t = 2.9$  ns) is consistent with the LASNEX calculation. However, the measured electron plasma temperature at  $t = 2.9$  ns is  $0.8 \pm 0.1$  keV, lower than the predicted 1.2 keV at this location. The error bars of the Mach 1 measurement are largest in the direction away from the foil due to the possibility that the beam was deflected by the plasma density gradient, with a maximum error defined by the spatial view of our diagnostic. Even with this effect, the error in the Mach 1 measurement is much smaller than the spatial and temporal extent of the region sampled in the main experiment.

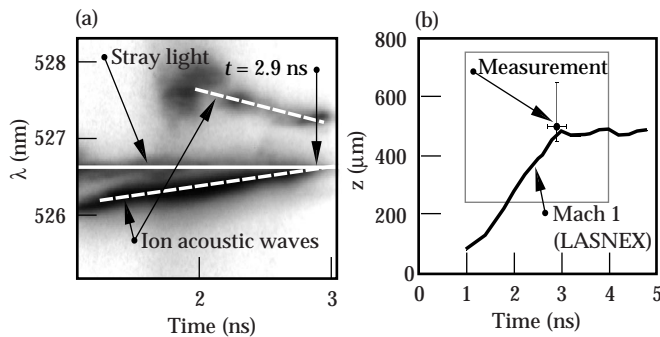


FIGURE 1. (a) Thomson scattering image from a  $\lambda = 526.6$ -nm probe focused at  $z = 500 \mu\text{m}$  from the original foil position, resolved in wavelength and in time. The upshifted ion acoustic wave feature overlaps the unshifted light at  $t = 2.9$  ns, signifying a Mach 1 plasma flow. (b) The LASNEX calculation of the Mach 1 flow location is plotted against time. The measurement from (a) is shown in comparison. The dotted box represents the typical spatial and temporal extent of the crossed beams in the primary experiment. (08-00-0798-1541pb01)

The main experiment was then performed by crossing two additional  $\lambda = 351$ -nm beams in the exploding foil plasma. We refer to the higher-intensity beam as the “pump” and the lower-intensity beam as the “probe.” As shown in Figure 2, these beams arrived from opposite directions, separated by an angle of  $152^\circ$ . Both the pump and probe were incident at  $14^\circ$  from the normal of the foil (the  $z$ -axis, defined in Figure 2), and the resultant ion wave was therefore aligned to the plasma flow along the  $z$ -axis. The pump and probe beams were originally focused at a location  $z = -500 \mu\text{m}$  from the  $z = 0$  initial foil position. The pump has a higher frequency in the frame of the flowing plasma on the  $-z$  half of the foil, and therefore the resonance would be expected to transfer energy from the pump to the probe and the ion wave.

The probe light transmitted through the plasma was incident on a frosted fused-silica plate 1.5 m from the target, and the scattered light was then imaged onto a fast photodiode.<sup>22</sup> Postprocessing of the photodiode signal helped correct for the finite-time response of both the large scatter plate and the diode. The final absolute uncertainty in the transmission measurements is  $\pm 14\%$  ( $\pm 20\%$  for time scales  $< 100$  ps), and the relative uncertainty between different shots is  $\pm 10\%$ .

The specifications of the crossing beams were as follows: the pump beam was identical to the heater beams (square pulse, 3 kJ in 3 ns, KPP), but arrived 1 ns late, staying on from  $t = 1$  ns to  $t = 4$  ns. The pump was focused to a 340- $\mu\text{m}$  full-diam spot, reaching an intensity of  $10^{15} \text{ Wcm}^{-2}$ . The probe beam had a typical energy of 0.2 kJ, and two focal spots were used. First, no phase plate was used on the probe, allowing a focused FWHM of 100  $\mu\text{m}$  (170- $\mu\text{m}$  full diameter). The probe’s pulse shape was a 3-ns upward ramp, beginning at  $t = 1$  ns and reaching a peak of 150 GW at  $t = 4$  ns.

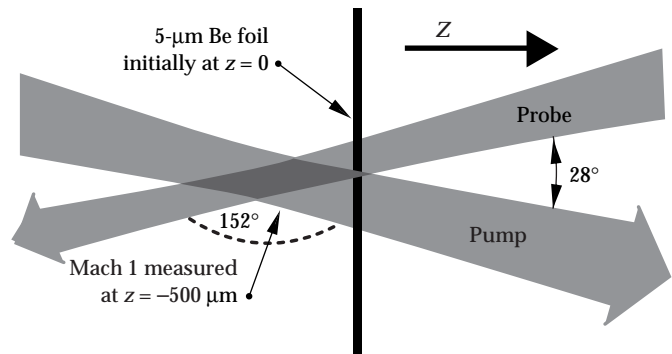


FIGURE 2. The experimental geometry is shown. The 5- $\mu\text{m}$  Be foil is initially at  $z = 0$ , where  $z$  is the normal to the foil in the direction of the “pump” beam propagation. At  $t = 0$  ns, two heater beams (not shown) illuminate the foil from both sides. At  $t = 1$  ns, the “pump” and “probe” laser beams intersect at a known distance from the foil, at a  $152^\circ$  angle. The diamond-shaped crossing region can have a  $z$ -extent of 850  $\mu\text{m}$  to 1300  $\mu\text{m}$  depending on the focal spot sizes, but  $> 75\%$  of the intensity intersects in a region only half this size. (08-00-0798-1542pb01)

## Results

The transmission of this probe beam is plotted against time in Figure 3a. With no pump beam present, the transmission of the probe through the exploding foil stabilized at 50–60%. With the addition of the pump beam, crossing the probe at a location  $z = -500 \mu\text{m}$ , the transmission of the probe increased to near 100% on short time scales. However, when the two beams were crossed at a location  $z = -750 \mu\text{m}$ , the probe transmission returned to the previous 50–60% level. Because the probe passed through the bulk of the exploding foil plasma before reaching the crossing region, this region had an average intensity ratio  $I_{\text{pump}}/I_{\text{probe}}$  of  $\sim 3$ .

To change this intensity ratio, a KPP was then added to the probe beam, increasing the spot size to  $340 \mu\text{m}$  (full diameter) and raising the average  $I_{\text{pump}}/I_{\text{probe}}$  to  $\sim 25$ . Also, the probe's pulse shape was changed to a 4-ns square pulse, extending from  $t = 1 \text{ ns}$  to  $t = 5 \text{ ns}$ . The increased size of the probe stretched the  $z$ -extent of the diamond-shaped region where the full beams intersected from  $850 \mu\text{m}$  to  $1350 \mu\text{m}$ . The length of the region where  $>80\%$  of the energy intersected increased from  $500 \mu\text{m}$  to  $800 \mu\text{m}$ .

Figure 3b shows the transmission of this lower-intensity probe beam, both with and without the pump beam. The no-pump transmission was nearly identical to the previous case despite the different pulse shapes, evidence that the low-intensity probe beam was not strongly affecting the plasma. With the pump beam present, the transmission was again increased to  $\sim 100\%$  levels when the beams were crossed at  $z = -500 \mu\text{m}$ ;  $\sim 80\%$  levels when the beams were crossed at the original foil position ( $z = 0$ ); and no significant transmission enhancement when the beams were crossed at  $z = +500 \mu\text{m}$ .

## Discussion

Increased transmission of the probe beam in the presence of a pump, however, is not by itself absolute evidence of energy transfer; alternatively, the pump might heat the plasma and thereby decrease the inverse bremsstrahlung absorption of the probe beam. LASNEX simulations show no pump beam effect on the plasma density or Mach 1 location, but do show a higher temperature plasma when the pump is on. This temperature change increases the peak theoretical probe transmission from 60% to 70%, but cannot explain the observed  $\sim 100\%$  transmission. In addition, this effect is calculated to occur late in the pump pulse, from  $t = 3 \text{ ns}$  onward, rather than the earlier  $t = \sim 2 \text{ ns}$  where our peak transmission is observed. Further evidence against this pump-heating scenario includes a measurement of the transmission of the pump beam; it peaks later in time ( $t = 3.2 \text{ ns}$ ), at a level of 55%, while the amplified probe signal peaks earlier ( $t = 2.4 \text{ ns}$ ) and with much higher transmission levels. Because the two

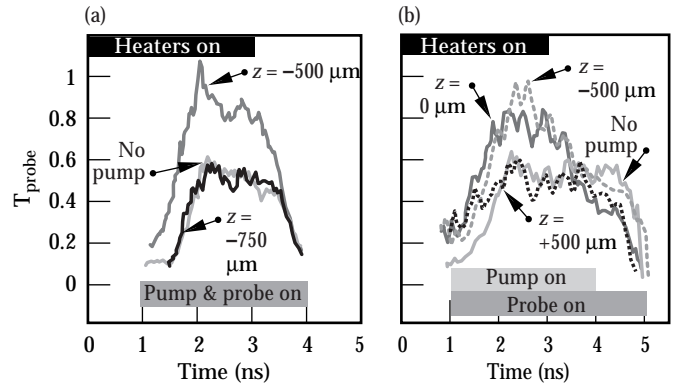


FIGURE 3. (a) Probe transmission fraction ( $T_{\text{probe}}$ ) is plotted against time for a pump/probe intensity ratio of  $\sim 3$ . The light gray solid line is the probe-only (no-pump) condition. The other data shows beam-crossing locations of  $z = -500 \mu\text{m}$  (dark gray solid line) and  $z = -750 \mu\text{m}$  (black line). (b) Probe transmission fraction is plotted against time for a pump/probe intensity ratio of  $\sim 25$ . The light gray solid line is the probe-only condition. The other data shows beam-crossing locations of  $z = -500 \mu\text{m}$  (dark gray dashed line),  $z = 0 \mu\text{m}$  (black solid line), and  $z = +500 \mu\text{m}$  (black dashed line). (08-00-0798-1543pb01)

beams are not exactly colinear, any pump-induced heating should have primarily increased the pump transmission.

For each transmission measurement, a linear gain factor can be computed by simply dividing the crossed-beam transmission by the no-pump transmission. Although the early-time peak gains are large ( $>3$ ) in both cases where the beams were crossed at  $z = -500 \mu\text{m}$ , the corresponding errors are large as well because of the lower no-pump transmission values at these times. A more quantitative gain measurement can be made by averaging the gain over  $2 \text{ ns} < t < 3 \text{ ns}$ , the time period when the Mach 1 flow velocity is calculated to be between  $z = -300 \mu\text{m}$  and  $z = -500 \mu\text{m}$ . These averages are plotted versus position in Figure 4. The large horizontal error bars represent the extent in the  $z$ -axis of the high-intensity diamond-shaped crossing region of the two beams. The maximum gain values of  $\sim 1.6$  occurred when the crossing region overlapped the Mach 1 region; little gain was observed when the beams were crossed outside this region. This dependence on position is strong evidence of a resonant process.

It is interesting to note that the measured average gain at  $z = -500 \mu\text{m}$  is roughly the same ( $\sim 1.6$ ) for both experimental intensity ratios. If the resonant ion wave were saturated, one would expect the gain to increase with increasing  $I_{\text{pump}}/I_{\text{probe}}$ . Our equal gain measurements, however, suggest that this process is not in a saturated regime. This conclusion concurs with previous resonant energy-transfer scaling<sup>8</sup> but is at odds with the near-complete transfer of the pump energy predicted by assuming a linearly driven ion wave in a homogeneous plasma.<sup>12,16</sup>

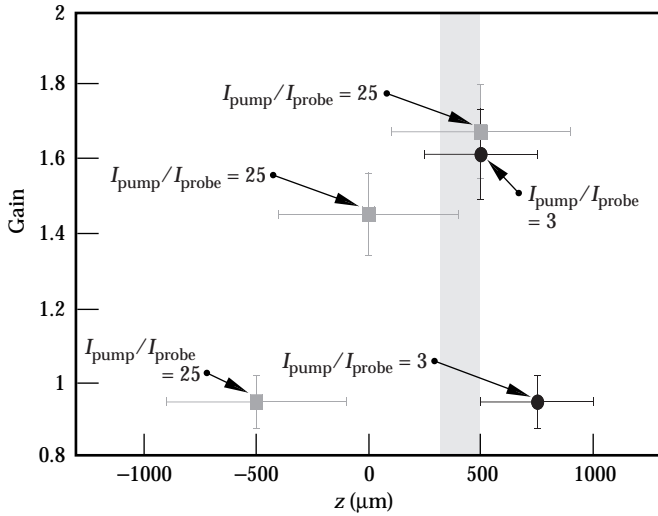


FIGURE 4. The gain factor of the probe beam (averaged from  $2 \text{ ns} < t < 3 \text{ ns}$ ) is plotted versus position for each crossed-beam location. Circles are for pump/probe intensity ratios of 3; squares are ratios of 25. The large horizontal error bars represent the region over which  $>80\%$  of the crossed beams overlap. The shaded region represents the calculated Mach 1 location during the  $2\text{-ns} < t < 3\text{-ns}$  period. (08-00-0798-1544pb01)

One mechanism that could explain the low energy transfer is a spatial degradation of gain due to velocity fluctuations produced by spatially inhomogeneous laser beams.<sup>8,16,23</sup> Laser “hot spots” can also modify the plasma’s electron distribution function, creating fluctuations in the ion-acoustic frequency,<sup>24</sup> which could further spatially detune the resonance condition in our experiment. Both of these effects would be enhanced by large-scale filamentation of the pump beam.<sup>25</sup>

Numerical simulations of such plasmas with strong gradients show further reductions of the amplification. BZOHAR, a 2D electromagnetic code that uses particle ions and Boltzmann fluid electrons,<sup>26</sup> has been used to perform simulations of this experiment on small spatial scales.<sup>27</sup> This suggests that the resonant ion waves and the probe amplification saturate after several ion acoustic periods, but the energy gain quickly relaxes (after 40 ps) and becomes nearly proportional to the input probe intensity, as seen in the experiments. BZOHAR arrives at this “linear” condition by means of nonlinear detuning and nonlinear localization of the ion-wave resonance.

## Summary

Enhanced transmission of a laser beam has now been observed when it is crossed with a higher-intensity beam of the same frequency in a flowing plasma. Positional and temporal scaling of this effect demonstrates that this is due to a resonance with an ion wave that has zero frequency in the laboratory frame, making this the first observation of steady-state energy transfer between identical frequency laser beams. The observed intensity gain of  $\sim 1.6$  in two different intensity regimes suggests that the resonant energy transfer is responding linearly to the driving laser beams.

## Notes and References

1. N. M. Kroll, A. Ron, and N. Rostoker, *Phys. Rev. Lett.* **13**, 83 (1964).
2. V. N. Tsytovich and A. B. Shvartsburg, *Sov. Phys. Tech. Phys.* **11**, 1431 (1967); L. M. Kovrizhnykh, *Sov. Phys. Tech. Phys.* **11**, 1183 (1967); V. Stefan, B. I. Cohen, and C. Joshi, *Science* **243**, 494 (1989).
3. B. L. Stansfield, R. Nodwell, and J. Meyer, *Phys. Rev. Lett.* **26**, 1219 (1971).
4. T. Tajima and J. M. Dawson, *Phys. Rev. Lett.* **43**, 267 (1979).
5. C. E. Clayton, C. Joshi, C. Darrow, and D. Umstadter, *Phys. Rev. Lett.* **54**, 2342 (1985).
6. C. E. Clayton et al., *Phys. Rev. Lett.* **70**, 37 (1993).
7. C. J. Pawley, H. E. Huey, and N. C. Luhmann, Jr., *Phys. Rev. Lett.* **49**, 877 (1982); C. W. Domier and N. C. Luhmann, Jr., *Phys. Rev. Lett.* **69**, 3499 (1992).
8. R. K. Kirkwood et al., *Phys. Rev. Lett.* **76**, 2065 (1996).
9. D. M. Villeneuve, H. A. Baldis, and J. E. Bernard, *Phys. Rev. Lett.* **59**, 1585 (1987).
10. A. K. Lal et al., *Phys. Rev. Lett.* **78**, 670 (1997).
11. V. V. Eliseev et al., *Phys. Plasmas* **3**, 2215 (1996).
12. C. J. McKinstrie, J. S. Li, R. E. Giacone, and H. X. Vu, *Phys. Plasmas* **3**, 2686 (1996).
13. I. M. Begg and R. A. Cairns, *J. Phys. D* **9**, 2341 (1976).
14. R. W. Short and E. A. Williams, *Phys. Rev. Lett.* **47**, 337 (1981); C. J. Randall, J. R. Albritton, J. J. Thomson, *Phys. Fluids* **24**, 1474 (1981); K. Baumgärtel and K. Sauer, *Phys. Rev. A* **26**, 3031 (1982); R. W. Short and E. A. Williams, *Phys. Fluids* **26**, 2342 (1983).
15. R. K. Kirkwood et al., *Phys. Plasmas* **4**, 1800 (1997); S. H. Glenzer et al., *Phys. Plasmas*, to be submitted.
16. W. L. Kruer et al., *Phys. Plasmas* **3**, 382 (1996).
17. C. J. McKinstrie et al., *Phys. Rev. E* **55**, 2044 (1997).
18. S. W. Haan et al., *Phys. Plasmas* **2**, 2480 (1995).
19. S. N. Dixit et al., *Optics Lett.* **21**, 1715 (1996).
20. G. Zimmerman and W. Kruer, *Comments Plasma Phys. Controlled Fusion* **2**, 85 (1975).
21. S. Glenzer et al., *Rev. Sci. Instrum.* **68**, 641 (1997).
22. J. D. Moody, et al., *Review of Sci. Instr.* **68**, 1725 (1997).
23. B. B. Afeyan et al., *Bull. Am. Phys. Soc.* **40**, 1822 (1995) and *Phys. Plasmas*, to be submitted; D. S. Montgomery et al., *Phys. Plasmas*, in press (1998).
24. B. B. Afeyan, A. E. Chou, and W. L. Kruer, *ICF Quarterly Report*, Lawrence Livermore National Laboratory, Livermore, CA (1997) and submitted to *Phys. Rev. E*; B. B. Afeyan et al., *Phys. Rev. Lett.*, **80**, 2322 (1998).
25. A. J. Schmitt and B. B. Afeyan, *Phys. Plasmas* **5**, 503 (1998).
26. B. I. Cohen et al., *Phys. Plasmas* **4**, 965 (1997).
27. B. I. Cohen et al., *Phys. of Plasmas* **5**, 3402 (1998).